Wavefront outer scale monitoring at La Silla

A. A. Tokovinin[a], A. Ziad[b], F. Martin[b], R. Avila[b],

J. Borgnino[b], R. Conan[b], M. Sarazin[c]

[a]Sternberg Astronomical Institute, Universitetsky prosp., 13, 119899 Moscow, Russia

[b] U.M.R. Astrophysique N^o 6525 - C.N.R.S. - Université de Nice-Sophia Antipolis, F-06108 Nice Cedex 2, France

[c]European Southern Observatory, Karl-Schwarzschild-Str. 2, D-85748, Garching bei München, Germany

ABSTRACT

The effective wavefront outer scale $\mathcal{L}_0$ was monitored continuously during 16 nights in August-September 1997 using the new Grating Scale Monitor (GSM) instrument. Simultaneous comparison with the data from open-loop adaptive optics system on the ESO 3.6 m telescope revealed a good agreement of the $\mathcal{L}_0$ derived by both methods. The GSM principle is similar to the Shack-Hartmann sensor: angle of arrival fluctuations are measured with four 10-cm telescopes and the outer scale is computed from their normalized covariances. The seeing and effective wavefront velocity are measured as well. GSM does not suffer from dome and mirror seeing effects and can be used anywhere for site evaluation.

Outer scale has log-normal distribution, its median is found to be 24 m, with a rms scatter of $\log \mathcal{L}_0$ of ± 0.22. Short isolated bursts of high $\mathcal{L}_0$ values were sometimes observed. A weak correlation of $\mathcal{L}_0$ and seeing angle exists for some nights.

Decametric values of $\mathcal{L}_0$ found here imply that at baselines of few meters the influence of finite $\mathcal{L}_0$ on the energy balance between tip-tilt and higher-order modes must be properly taken into account. This can sensibly modify the predicted performance of adaptive optics systems.

Keywords: atmospheric turbulence, seeing, adaptive optics, interferometry, outer scale

1. INTRODUCTION

The knowledge of the parameters of the optical turbulence in the atmosphere is essential for all high angular resolution techniques, e.g. adaptive optics (AO) and optical interferometry.[1] These parameters include the Fried coherence radius r_0, atmospheric time constant τ_0, isoplanatic angle θ_0 and the wavefront outer scale $\mathcal{L}_0$. This latter parameter was poorly known until recently. Here we present the first results of $\mathcal{L}_0$ monitoring at a major astronomical site during 16 nights.

The definition of $\mathcal{L}_0$ is related to the behaviour of the wavefront phase structure function $D_\phi(r)$. If for large r $D_\phi(r)$ saturates at a level $2\sigma_\phi^2$ (σ_ϕ^2 being phase variance), then $\mathcal{L}_0$ is defined as the distance where the extrapolated Kolmogorov phase structure function reaches this level:

$$6.88(\mathcal{L}_0/r_0)^{5/3} = 2\sigma_\phi^2. \tag{1}$$

The *wavefront outer scale* $\mathcal{L}_0$ can be represented as a weighted average of *turbulence outer scales* L_0 in the individual atmoshperic layers along a propagation path.[2] As shown by Lukin et al.,[3] the real phase structure

A.A.T.: E-mail: toko@sai.msu.su
A.Z.: E-mail: aziz@procyon.unice.fr
F.M.: E-mail: martin@boulega.unice.fr

function resulting from a combination of layers with different L_0 can be reasonably well approximated by a single "effective" outer scale, although its particular value depends on the baselines under consideration.

The saturation of $D_\phi(r)$ is actually never observed, so the definition (1) is of little practical use. Different heuristic models were proposed to describe the behaviour of the $D_\phi(r)$ in the transition region between the inertial range and the saturation. In the interpretation of our data we use the Von Kàrmàn turbulence model for which the spatial spectrum of the phase fluctuations can be written as

$$W_\phi(f) = 0.0228 r_0^{-5/3} (f^2 + \mathcal{L}_0^{-2})^{-11/6}, \tag{2}$$

where r_0 is the Fried parameter and $\mathcal{L}_0$ is the wavefront outer scale. The $\mathcal{L}_0$ values provided by GSM can be viewed as the values of Von Kàrmàn model parameter $\mathcal{L}_0$ that approximates $D_\phi(r)$ at metric baselines. If another model is used, it is important that its outer scale parameter satisfies (1), otherwise it would be impossible to intercompare different results.

The important deviation of $D_\phi(r)$ from Kolmogorov law occurs already at baselines $r \approx \mathcal{L}_0/10$. Decametric values of $\mathcal{L}_0$ reported below imply that AO systems with apertures above 1 m are subject to outer scale effects. For finite $\mathcal{L}_0$ the energy of wavefront perturbations is transferred to higher order modes. For a given r_0 the performance of AO system working on natural stars is degraded, as well as its isoplanatic angle, but a reduced amount of tip-tilt correction can improve the performance of a laser guide star AO system.[4–6]

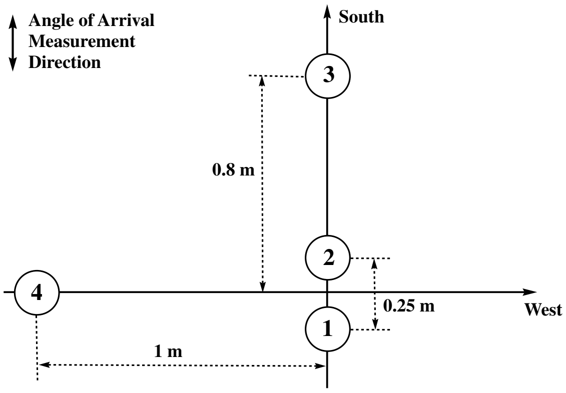

Figure 1. Geometrical layout of the GSM instrument at La Silla.

2. THE GSM INSTRUMENT

Our approach to measuring $\mathcal{L}_0$ consists in the evaluation of the covariance between the angle of arrival fluctuations at two locations on the wavefront. If the direction of angle measurement is parallel to the baseline, the *longitudinal* covariance is obtained, which is roughly proportional to the second derivative of $D_\phi(r)$ over r. Thus, when $D_\phi(r)$ passes from the Kolmogorov growth to saturation, its second derivative and the longitudinal covariance become negative. These qualitative arguments apply for arbitrary baseline orientation. By measuring the angle of arrival covariance C_α at different baselines and adjusting the model parameter we estimate $\mathcal{L}_0$. The dependence of C_α on the baseline length B, angle γ between measurement direction and the baseline, telescope aperture diameter D, outer scale $\mathcal{L}_0$ and the Fried parameter r_0 for Von Kàrmàn model is given by the following integral[7]:

$$C_\alpha(B,\gamma,D,\mathcal{L}_0) = 0.0716 \lambda^2 r_0^{-5/3} \int_0^\infty \mathrm{d}f f^3 (f^2+\mathcal{L}_0^{-2})^{-11/6} [J_0(2\pi f B) - \cos(2\gamma) J_2(2\pi f B)] [2J_1(\pi f D)/(\pi f D)]^2, \tag{3}$$

where J_i are the i-th order Bessel functions of the first kind.

The Grating Scale Monitor (GSM) uses four 10-cm telescopes pointed to the same star. In each telescope the angle of arrival in one direction is measured by rapid modulation of stellar image falling onto a Ronchi grating and by the real-time processing of the transmitted light.[8] Simultaneous estimates of angle of arrival are obtained with a 5 ms sampling rate from which the covariances are computed. First measurements of $\mathcal{L}_0$ with this instrument are published by Agabi et al.[9] GSM can be viewed as a Shack-Hartmann sensor which operates without a large telescope and explores the wavefront structure on metric scales. Its data are not contaminated by dome or mirror seeing.

The angle of arrival covariance depends not only on $\mathcal{L}_0$ but also on the Fried parameter r_0. This is why we install 2 telescopes on a common mounting and estimate r_0 from the differential image motion variance σ_d^2, using the well known DIMM principle.[10,11] All measured covariances are normalized by σ_d^2 in order to eliminate the dependence on r_0 and compared to the grid of pre-calculated normalized covariances. With 4 telescopes we have 6 baselines which provide 6 estimates of $\mathcal{L}_0$; a median of these is taken as a final outer scale value. We checked that the direct least-squares adjustment of $\mathcal{L}_0$ to fit the measured covariances leads to almost the same results. The projection effects are taken into account in data reduction: baselines and angle measurement direction are projected onto the sky before comparison with theoretical covariance grid. Data are processed immediately after the acquisition, permitting a quasi real-time monitoring of $\mathcal{L}_0$.

A common problem in angle of arrival (AA) measurements is related to possible telescope vibrations and imperfect guiding. GSM measures AA in the declination direction to minimize telescope tracking errors. A second order polynomial is fitted to the measured AA $\alpha(t)$ and subtracted in order to eliminate possible low-frequency contamination by mechanical errors. The high frequency contribution due to wind-induced vibration does not influence the differential variance σ_d^2. We assume that telescope vibrations are mutually uncorrelated and do not distort the covariances. An independent control of telescope vibration amplitude is provided by the comparison of r_0 as calculated from σ_d^2 with r_{0i} calculated for the i-th telescope from the angle of arrival dispersion and corrected for the finite outer scale using the relation[12]

$$\sigma_\alpha^2 = 0.179\lambda^2 D^{-1/3} r_0^{-5/3}[1 - 1.52(D/\mathcal{L}_0)^{1/3}]. \tag{4}$$

For the data set discussed below the vibrations are not apparent even at wind speed of 15 m/s.

The scintillation index σ_I^2 with 5 ms integration time can be computed from the GSM data to give the rough idea of the high-altitude turbulence strength and the isoplanatic angle.[13] In addition, we can estimate the effective wind speed and direction from the time delays at perpendicular bases. Thus, GSM can potentially provide the information on all turbulence parameters relevant to adaptive optics and interferometry.

3. LA SILLA MISSION

Monitoring of $\mathcal{L}_0$ at the La Silla observatory (Chile) was performed from August 27 to September 19 1997, in the framework of the ESO VLT Astronomical Site Monitor development program. The 3 equatorial mounts with GSM telescopes were installed on 3 piers: two differential telescopes on a central pier and two remaining telescopes with their mounts on two piers to the south and east of the central pier at the distances of 0.8 and 1 meters, respectively (Fig. 1). These baselines were chosen for optimal sensitivity to the $\mathcal{L}_0$. The height of GSM telescopes above the ground was 1.7 m. GSM was located near the ESO DIMM instrument,[10] approximately at the center of the mountain ridge. With the prevailing wind from the north this location should be free from local disturbances. Standard data acquisition sequence consisted of 2 minute integrations repeated every 4 minutes continuously during the night, with some gaps due to source change, cloud passages, etc.

Additional data on temperature, humidity, wind direction and speed near ground were taken from the ESO meteorological service. The seeing measured by the ESO DIMM is also available for comparison with GSM. Satellite images and wind maps at 200 mB were used for the assessment of the general meteorological situation. Most of the time the jet stream passed over La Silla. By consequence, the seeing was worse than average (median value 1.7″, accompanied by a strong wind and scintillation.

4. TEMPORAL BEHAVIOUR OF THE OUTER SCALE

A typical temporal evolution of $\mathcal{L}_0$ during one night is shown in Fig. 2. A slow variation of $\mathcal{L}_0$ is usually observed, as well as isolated "bursts" of high outer scale. These bursts are noted here for the first time. They are typical of our data set, being more frequent on some nights, less frequent or absent on some other nights. Burst duration is few minutes, usually they are observed as one isolated high value of $\mathcal{L}_0$, rarely as two adjacent values.

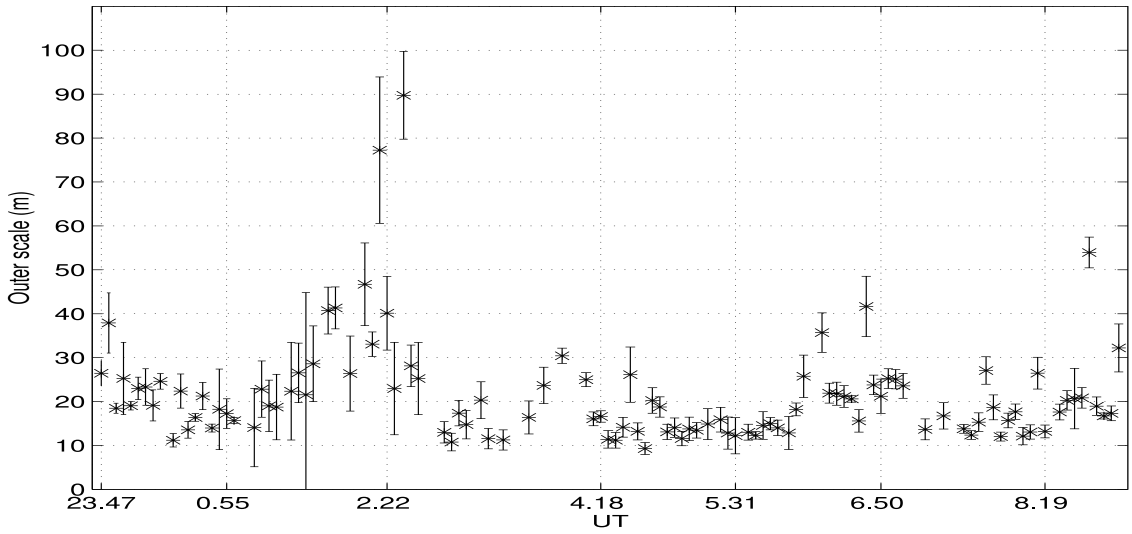

Figure 2. Temporal evolution of the wavefront outer scale $\mathcal{L}_0$ during the night of September 15/16. The error bars corresponding to the $\pm\sigma$ uncertainity were calculated from the scatter of $\mathcal{L}_0$ found for 6 different baselines.

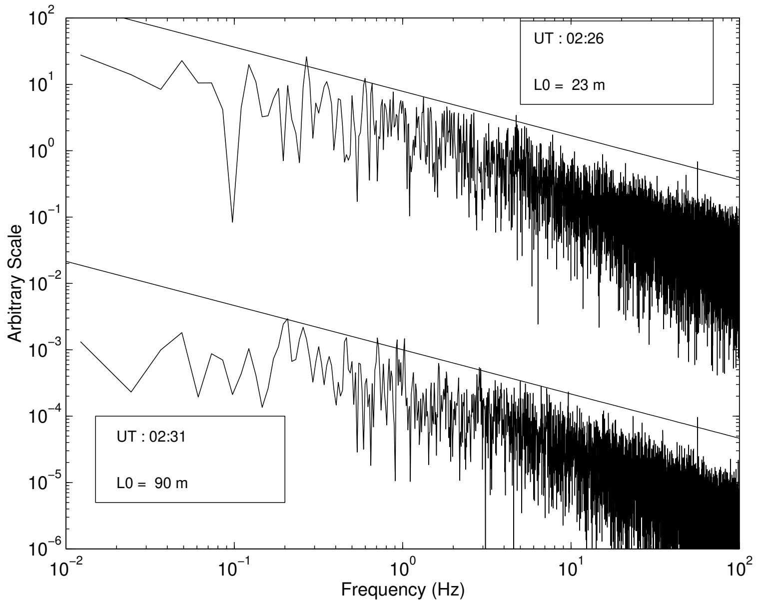

Figure 3. Temporal cross-power spectra of angle of arrival fluctuations recorded at 25 cm baseline for two consecutive 2-min data acquisitions corresponding to different $\mathcal{L}_0$ (the night of September 15/16). A $-2/3$ logarithmic slope is indicated by straight lines. Arbitrary vertical shift was introduced to separate the spectra. No significant difference in the shape of temporal spectra corresponding to different $\mathcal{L}_0$ can be seen.

The angle of arrival cross power spectrum calculated for any baseline typically shows the $-2/3$ slope at intermediate frequencies corresponding to the developed turbulence in the inertial range[7] (Fig. 3). We looked for the difference of the temporal cross-spectra corresponding to the different $\mathcal{L}_0$ and have not found any convincing evidence of them. A weak correlation between $\mathcal{L}_0$ and seeing exists for some (but not all) nights, as illustrated in Fig. 4. A correlation between nightly median values of $\mathcal{L}_0$ and seeing is rather evident, as well as $\mathcal{L}_0$ correlation with median ground wind speed (Fig. 5).

In Fig. 6 we plot the median values of $\mathcal{L}_0$ for each night with the bars comprising 80% of nightly values. It can be seen that average outer scale and its scatter do change from night to night. The overall distribution of $\mathcal{L}_0$ appears to be log-normal with a median of 24 m and a rms scatter of ±1.67 times from the median.

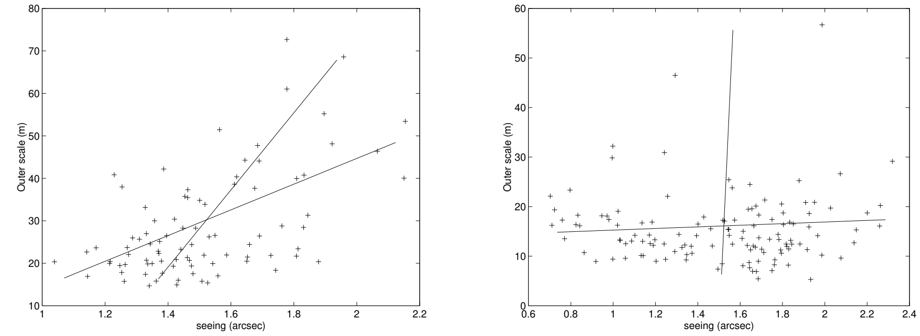

Figure 4. Wavefront outer scale $\mathcal{L}_0$ plotted against seeing angle for the nights of September 6/7 (left) and August 28/29 (right), together with the regression lines. Correlation coefficients are 0.55 and 0.01, respectively.

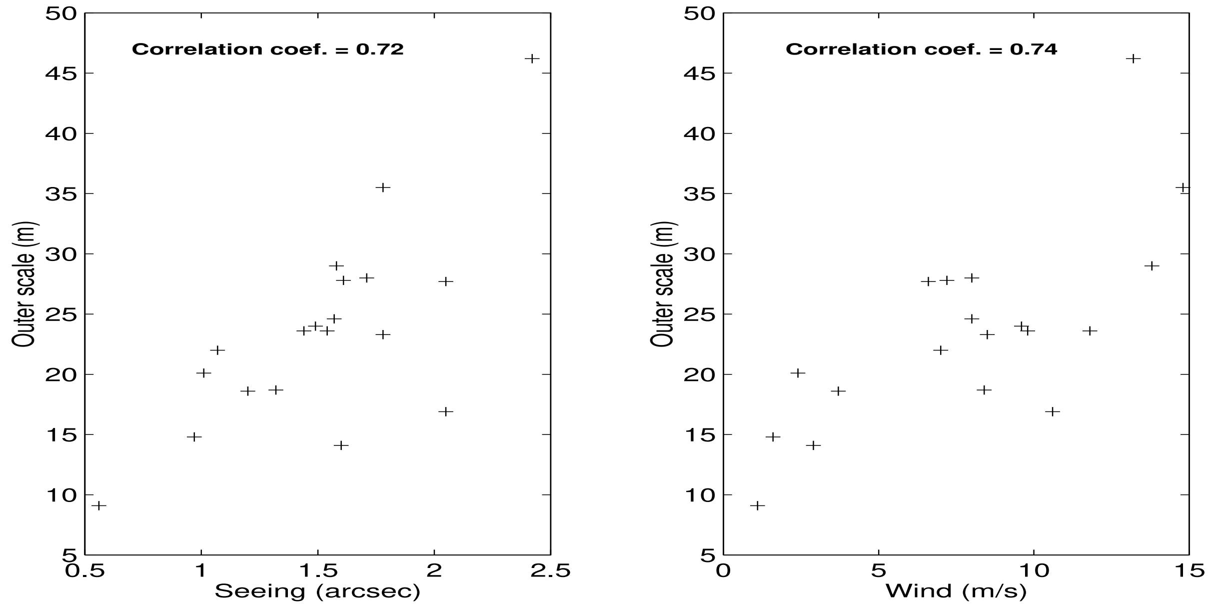

Figure 5. The correlation of nightly median values of $\mathcal{L}_0$ with median seeing and median ground wind speed.

It is interesting to note that the typical outer scale values are not very much different from the prediction of those turbulence models which assume that $L_0(h)$ in meters is equal to $2\sqrt{h[\mathrm{m}]}$.[14] The seeing is usually dominated by the lowest kilometer of the atmosphere with the attendant decametric outer scales.

5. COMPARISON WITH ADONIS

On the night of August 29/30 the data on wavefront statistics were recorded with the ADONIS AO system[15,16] on the 3.6 m ESO telescope during 1 hour. It worked with open servo loop. The AA variances on the individual Shack-Hartmann wavefront sensor sub-apertures and on the full telescope aperture were computed. Their ratio is used to derive $\mathcal{L}_0$ from Eq. (4). This method was first suggested in.[12] Of course, this approach is valid only when other sources of AA fluctuations, e.g. telescope tracking errors, can be neglected.

In Fig. 7 the simultaneous estimates of $\mathcal{L}_0$ and seeing with ADONIS and GSM are compared. The good agreement between these two instruments can be seen. Notably, ADONIS data also show typical decametric $\mathcal{L}_0$ values together with short bursts. However there is no detailed correlation between the two instruments because they were separated by more than 1 km and the altitudes were different. The agreement between the estimates of $\mathcal{L}_0$ which were obtained independently of each other and using different techniques is encouraging.

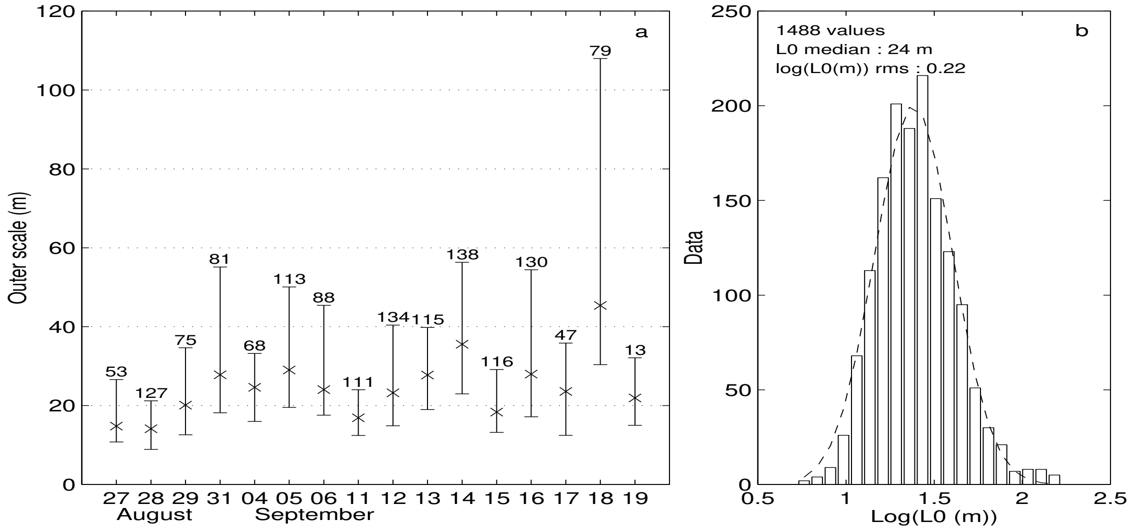

Figure 6. Summary of the outer scale statistics during 16 nights. On the left pannel (a) the median values of $\mathcal{L}_0$ are plotted as crosses, the variation range is indicated by bars which comprise 80% of nightly values (10 and 90 percentile levels of cumulative distribution). The total number of measurements on each night is indicated. On the right pannel (b) the histogram of log$\mathcal{L}_0$ is plotted, with a fitted log-normal distribution in dashed line.

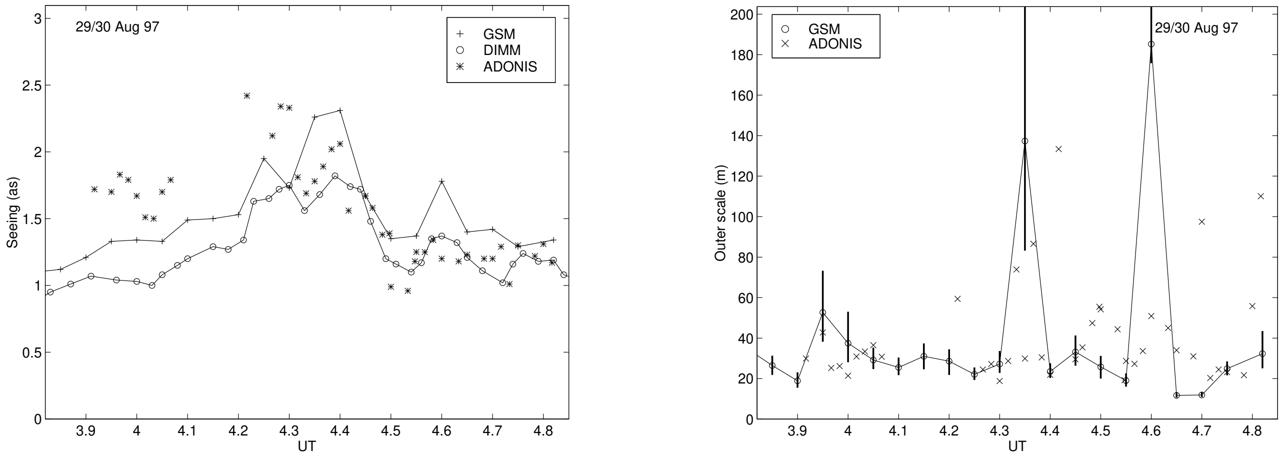

Figure 7. Comparison of the simultaneous measurements with GSM and with ADONIS AO system during 1 hour on August 29/30. Left: seeing as measured by GSM, ADONIS and ESO DIMM. Right: wavefront outer scale measured by GSM (circles with error bars) and ADONIS (crosses).

6. TEMPORAL EVOLUTION OF THE WAVEFRONT

In attempt to characterize the temporal properties of the perturbed wavefront, we analyzed the temporal cross-correlation functions of AA fluctuations at different baselines (Fig. 8). They present typically a peak displaced from the coordinate origin due to the wind delay. The width of the peak increases with baseline. Combining all shifts, we can determine the “effective” wavefront velocity and its direction which for this example was 8.3 m/s, NNE (the ground wind speed as measured by ESO meteorological service was 3.7 m/s from North). The corresponding time constant of adaptive optics as defined by[17] is 3.2 ms ($\lambda = 0.5$ nm).

In situations when there is a well-defined single dominant layer containing most of turbulent energy the wavefront

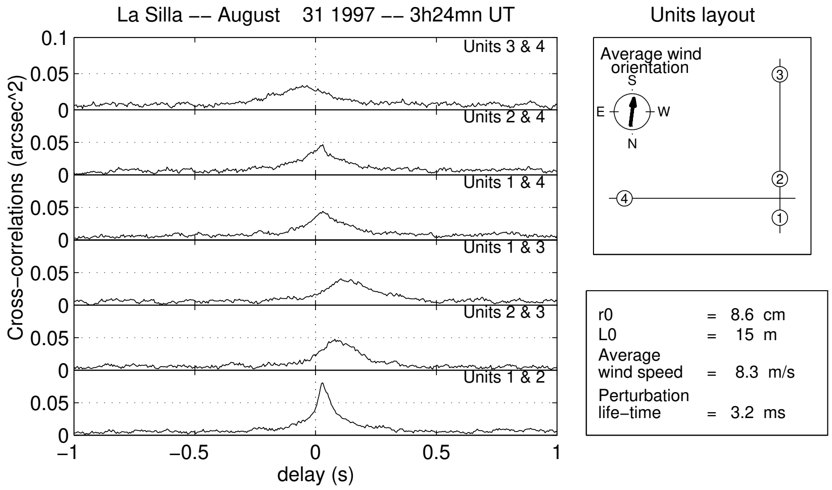

Figure 8. Temporal cross-correlation of angle of arrival fluctuations on all 6 GSM baselines. The positions of the cross-correlation peaks' maxima were used to estimate the projection of the effective wavefront velocity onto each baseline and to reconstruct the velocity vector.

temporal behaviour can be approximated by a single effective velocity. It is often the boundary layer that makes major contribution to seeing degradation. The derived wavefront speed and direction indeed were often not much different from the ground wind. The similar conclusion was reached in[18] from the analysis of ADONIS wavefront sensor data. It was noted there that the situations when a single effective wind speed describes adequately the wavefront evolution are not very typical (15% of cases). During our mission the seeing was worse than average due to the strong wind, and we may suppose that a dominant contribution of the boundary layer was more marked. The cross-correlation functions sometimes did not display well-defined peaks, and single-layer model was then not adequate.

7. CONCLUSIONS

For the first time the wavefront outer scale $\mathcal{L}_0$ was monitored continuously over several nights at a major astronomical site. The distribution of $\mathcal{L}_0$ appears to be log-normal, with median value of 24 m and a 1σ scatter of ± 1.67 times. Large isolated values of $\mathcal{L}_0$ are observed regularly and are possibly related to the moments of turbulent energy injection. GSM data are confirmed by independent wavefront measurements with a working AO system.

Our results indicate that the wavefront statistics deviates significantly from Kolmogorov law at baselines of a few meters. This fact is important for the calculation of AO systems performance.

The GSM instrument provides also data on the Fried parameter r_0 and the effective wavefront translation speed which is related to the AO time constant. Thus it is a promising instrument for the complete characterisation of astronomical site for high-resolution imaging techniques.

ACKNOWLEDGMENTS

The authors would like to thank the La Silla staff for the efficient support of our mission and all the people of Departement d'Astrophysique de l'Université de Nice and of O.C.A. (Observatoire de la Cote d'Azur) who helped us to prepare this measurement campaign. Financial support for this work came from INSU (Institut National des Sciences de l'Univers), french M.E.N.R.T. (Ministère de l'Education Nationale, de la Recherche et de la Technologie), and from ESO (European Southern Observatory).

REFERENCES

1. F. Roddier, "Effects of atmospheric turbulence in optical astonomy," in *Progress in Optics*, E. Wolf, ed., pp. 281–376, North Holand Publ. Co., Amsterdam, 1981.
2. J. Borgnino, "Estimation of the spatial coherence outer scale relevant to long baseline interferometry and imaging in optical astronomy," *Appl. Opt.* **29**, pp. 1863–1865, 1990.

3. V. P. Lukin, E. V. Nosov, and B. V. Fortes, “Effective outer scale of atmospheroc turbulence,” *Optica Atmosphery y Okeana (in russian)* **10**, pp. 162–171, 1997.
4. D. M. Winker, “The effect of a finite outer scale on the Zernicke decomposition of atmospheric turbulence,” *J. Opt. Soc. Amer.* **A8**, pp. 1568–1573, 1991.
5. R. J. Sasiela and J. D. Shelton, “Transverse spectral filtering and Mellin transform techniques applied to the effect of outer scale on tilt and tilt anisoplanatism,” *J. Opt. Soc. Amer.* **A10**, pp. 646–660, 1993.
6. V. V. Voitsekhovich and S. Cuevas, “Adaptive optics and the outer scale of turbulence,” *J. Opt. Soc. Amer.* **A12**, pp. 2523–2531, 1995.
7. R. Avila, A. Ziad, J. Borgnino, F. Martin, A. Agabi, and A. Tokovinin, “Theoretic spatiotemporal analysis of angle of arrival induced by atmospheric turbulence as observed with the grating scale monitor experiment,” *J. Opt. Soc. Amer.* **A14**, pp. 3070–3082, 1997.
8. F. Martin, A. Tokovinin, A. Agabi, J. Borgnino, and A. Ziad, “G.S.M.: a grating scale monitor for atmospheric turbulence measurements. I. The instrument and first results of angle of arrival measurements,” *Astron. Astrophys. Suppl. Ser.* **108**, pp. 1–8, 1994.
9. A. Agabi, J. Borgnino, F. Martin, A. Tokovinin, and A. Ziad, “G.S.M.: a grating scale monitor for atmospheric turbulence measurements. II. First measurements of the wavefront outer scale at O.C.A.,” *Astron. Astrophys. Suppl. Ser.* **109**, pp. 557–562, 1995.
10. M. Sarazin and F. Roddier, “The ESO differential image motion monitor,” *Astron. Astrophys.* **227**, pp. 294–300, 1990.
11. H. M. Martin, “Image motion as a measure of seeing quality,” *Publ. Astron. Soc. Pacif.* **99**, pp. 1360–1370, 1987.
12. A. Ziad, J. Borgnino, F. Martin, and A. Agabi, “Experimental estimation of the spatial-coherence outer scale from a wavefront statistical analysis,” *Astron. and Astrophys.* **282**, pp. 1021–1033, 1994.
13. G. Loos and C. Hogge, “Turbulence of the upper atmosphere and isoplanatism,” *Appl. Opt.* **18**, pp. 2654–2661, 1979.
14. R. E. Good, R. R. Beland, E. A. Murphy, J. H. Brown, and E. M. Dewan, “Atmospheric models of optical turbulence,” *SPIE* **928**, pp. 165–186, 1988.
15. F. Rigaut, G. Rousset, P. Kern, J. Fontanella, J. P. Gaffard, F. Merkle, and P. Lena, “Adaptive optics on a 3.6 m telescope: results and performance,” *Astron. Astrophys.* **250**, pp. 280–290, 1991.
16. J.-L. Beuzit, N. Hubin, E. Gendron, L. Demailly, P. Gigan, F. Lacombe, F. Chazalet, D. Rabaud, and G. Rousset, “ADONIS: a user-friendly adaptive optics system for the ESO 3.6 m telescope,” *SPIE* **2001**, pp. 955–960, 1994.
17. F. Roddier, J. Gilli, and G. Lund, “On the origin of speckle boiling and its effects in stellar speckle interferometry” *J. Opt. (Paris)* **13**, pp. 263–271, 1982.
18. E. Gendron and P. Lena, “Single layer atmospheric turbulence demonstrated by adaptive optics observations,” *Astrophys. Space Sci.* **239**, pp. 221–228, 1996.